DALTON
FULL PAPER

The structural chemistry of organotin derivatives of 5-mercapto-3-phenyl-1,3,4-thiadiazoline-2-thione: supramolecular structures involving intermolecular Sn · · · S, N–H · · · S or S · · · S interactions †

Vasile Berceanc,[a] Crina Crainic,[b] Ionel Haiduc,[b] Mary F. Mahon,[c] Kieran C. Molloy,[c] Monica M. Venter *[b,c] and Paul J. Wilson[c]

[a] *Department of Chemistry, Technical University of Timisoara, RO-1900 Timisoara, Romania*
[b] *Department of Chemistry, "Babes-Bolyai" University of Cluj, RO-3400 Cluj-Napoca, Romania*
[c] *Department of Chemistry, University of Bath, Bath, UK BA2 7AY*

Received 24th October 2001, Accepted 25th January 2002
First published as an Advance Article on the web 19th February 2002

Seven new organotin complexes of 5-mercapto-3-phenyl-1,3,4-thiadiazoline-2-thione (**I**), $R_nSn(PhN_2C_2S_3)_{4-n}$ [n = 1, R = Bu (**1**); n = 2, R = Ph (**2**), Bu (**3**), Me (**4**) and n = 3, R = Ph (**5**), Bu (**6**), Me (**7**)], along with the 4,4′-bipy and 4-$PyNH_2$ adducts of **7**, $[Me_3Sn(PhN_2C_2S_3)]_2$·(4,4′-bipy) (**8**) and $[Me_3Sn(4\text{-}PyNH_2)_2]^+[PhN_2C_2S_3]^-$ (**9**), respectively, have been synthesised. The coordination behaviour of **I** in **1**–**8** ranges from S(1) monodentate to S(1) + S(3) bidentate bridging, while the crystal structure of **9** contains the ligand as a non-bonded anion. The supramolecular structures of **2**, **7** and **8** have been found to consist of 1-D molecular chains built up by Sn · · · S (**7**) or S · · · S (**2**, **8**) intermolecular linkages. Additionally, the 1-D polymers of **7** aggregate in 'ribbon'-type double chains through S · · · S interactions and further self-organise *via* Ph · · · Ph face-to-face π-stacking, leading to a 3-D network. Extended intermolecular N–H · · · S interactions in the crystal lattice of **9** link the molecules in a 3-D network.

Introduction

We have an on-going interest in tin–sulfur chemistry, partly from the aspect of materials science, where we have investigated precursors for the deposition of tin sulfides,[1–3] and also because of the supramolecular assemblies which can be formed from such species.[4,5] It is the latter which forms the focus of this paper.

Supramolecular organometallic chemistry is a topical aspect of current research.[6] Our contributions to date have included the coordination behaviour of five- and six-membered thiol/thione heterocycles, and, specifically, the structures of their organotin and lead complexes.[4,5,7] For example, organotin-substituted tetrazole thiolates are known to adopt monomer,[7,8] trimer,[9] polymer[10] and sheet[4] structures, all containing σ-Sn–ligand bonds. In contrast, Ph_3PbSCN_4Ph has an intriguing lattice arrangement in which a tetrazole appears to approach a neighbouring lead in a π-coordinating manner.[11] Moreover, we have lately become interested in well-known analytical reagents as potential donors (*e.g.* trithiocyanuric acid), as very little is known of the synthesis and/or structural characterisation of their organometallic complexes.

The aim of this work was to elucidate the structures of new organotin derivatives of 5-mercapto-3-phenyl-1,3,4-thiadiazoline-2-thione (**I**) (also referred to in older literature as Bismuthiol II). Compound **I**, which can exist in either thiol (**Ia**) or thione (**Ib**) forms, has been intensively investigated as a precipitating agent[12–15] and its industrial importance has also been noted.[16]

The synthesis and spectral characterisation of some transition metal complexes of Bismuthiol II and related heterocycles (*e.g.* Bismuthiol I) has been carried out previously and S(1) + S(3) bidentate bridging coordination by the ligand has been suggested, despite the lack of any conclusive crystallographic support.[16–18] To our knowledge, very few organotin derivatives of **I** have been studied and no structural characterisations of such species have been reported so far.[19]

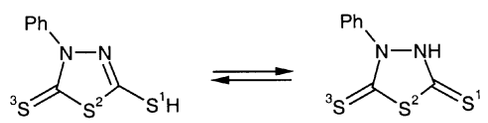

Ia **Ib**

Ligands such as **I** also present a number of opportunities for creating supramolecular arrangements. In addition to intermolecular bridging from Lewis base sites (either nitrogen or sulfur) and/or potential H-bonding from inclusion of solvents such as water or alcohol, the presence of a plethora of sulfur atoms can also gives rise to S · · · S interactions. Among the explosion of studies involving crystal engineering in recent years, these S · · · S interactions, being the weakest of the three classes listed above, have been largely ignored, save for those involving tetrathiafulvalene (TTF) and its analogues.[20] Such planar, sulfur-rich species are central to a large number of charge-transfer organic metals, and although π-stacking of planar donors and acceptors is the key structural feature in their one-dimensional conductivity, weak intermolecular S · · · S interactions often reduce this electronic anisotropy to two-dimensions. We herein report the role of each of the three lattice building strategies, including S · · · S bonding, in the supramolecular chemistry of the organotin derivatives of **I**.

Results and discussion

Synthesis and spectroscopy

Seven new organotin derivatives of **I**, $R_nSn(PhN_2C_2S_3)_{4-n}$ [n = 1, R = Bu (**1**); n = 2, R = Ph (**2**), Bu (**3**), Me (**4**) and n = 3, Ph (**5**),

† Electronic supplementary information (ESI) available: discussion of the spectral data. See http://www.rsc.org/suppdata/dt/b1/b109726a/

 DOI: 10.1039/b109726a

Bu (**6**), Me (**7**)], have been synthesised by direct reaction of the corresponding organotin chlorides and the potassium salt of **I** ($PhN_2C_2S_3K$) [eqn. (1)]. Further reaction of **7** with a large

$$R_nSnCl_{4-n} + (4-n)\,PhN_2C_2S_3K \longrightarrow R_nSn(PhN_2C_2S_3)_{4-n} + (4-n)\,KCl \quad (1)$$

$n = 1$, R = Bu (**1**);
$n = 2$, R = Ph (**2**), Bu (**3**), Me (**4**);
$n = 3$, R = Ph (**5**), Bu (**6**), Me (**7**).

excess of 4,4′-bipy or 4-$PyNH_2$ in diethyl ether results in the formation of a dinuclear adduct, $[Me_3Sn(PhN_2C_2S_3)]_2\cdot$(4,4′-bipy) (**8**), and a fully ionic species, $[Me_3Sn(4\text{-}PyNH_2)_2]^+$-$[PhN_2C_2S_3]^-$ (**9**), respectively [eqn. (2, 3)]. All derivatives **1**–**9** are

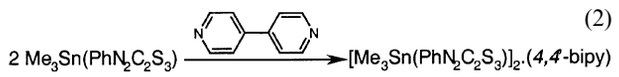

(2)

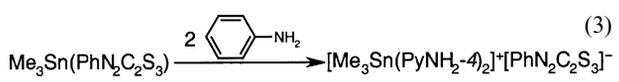

(3)

air stable in the solid state. Compound **6** was obtained as pale yellow oil which turned into a crystalline solid at low temperature. Compounds **1**–**8** are soluble in common organic solvents excepting hexane (**1**–**5**, **7**, **8**), while the insolubility of **9** can be explained by its ionic character. Recrystallisation from thf–hexane (**1**–**4**), diethyl ether–hexane (**5**, **7**) or diethyl ether (**8**) gave the products as pale yellow (**1**–**4**) or colourless (**5**–**9**) crystalline solids. Synthesis of **9** yielded the product as a colourless crystalline solid of analytical purity directly, without recourse to further purification.

A discussion of the spectral data associated with **1**–**9** is available as ESI. †

Structural chemistry

Suitable crystals for X-ray diffraction analysis were grown from thf–hexane (**1**–**3**) or diethyl ether–hexane (**7**) at room temperature, or from diethyl ether solution at low temperature (**8**). Due to the insolubility of **9**, crystals of satisfactory quality were obtained by slow diffusion of diethyl ether solutions of the two starting materials at room temperature over a period of one week.

Compound 1. The molecular structure of **1** (Fig. 1) consists of discrete monomers containing distorted tetrahedral $CSnS_3$ centres. The tin atom is directly bonded to the thiol groups (C–S) of **I**, the Sn–S distances [2.4523(7)–2.4687(7) Å] falling in the Sn–S bond length range determined previously for organotin trithiotriazines [2.435(3)–2.4708(8) Å].[5] The C–Sn–C bond angles [115.40(4)–118.59(8)°] are slightly larger, while the S–Sn–S angles [95.83(2)–105.75(2)°] are somewhat smaller when compared to the ideal value of 109.5°. This structural feature can be explained by the very weak anisobidentate chelation of two $PhN_2C_2S_3$ ligands through the ring nitrogen atoms [Sn(1) ··· N(1): 2.773(2), Sn(1) ··· N(3) 2.891(2) Å]. Such chelation was not observed for the third ligand, its ring nitrogen being placed at a distance of 4.23 Å from the metal centre. Within the four-membered SSnNC chelate rings, the shortening of the Sn ··· N distance leads to a marginal increase in the C–Sn–S bond angle [C(1)–Sn(1)–S(1): 118.59(8); C(1)–Sn(1)–S(4) 117.4(8)°] and a simultaneous decrease in the C–S–Sn angle by *ca.* 2° [C(5)–S(1)–Sn(1): 90.49(8); C(13)–S(4)–Sn(1) 92.68(8)°]. Moreover, the smallest S–Sn–S angle occurs between the two Sn–S bonds involved in the chelate rings [S(1)–Sn(1)–S(4): 95.83(2)°].

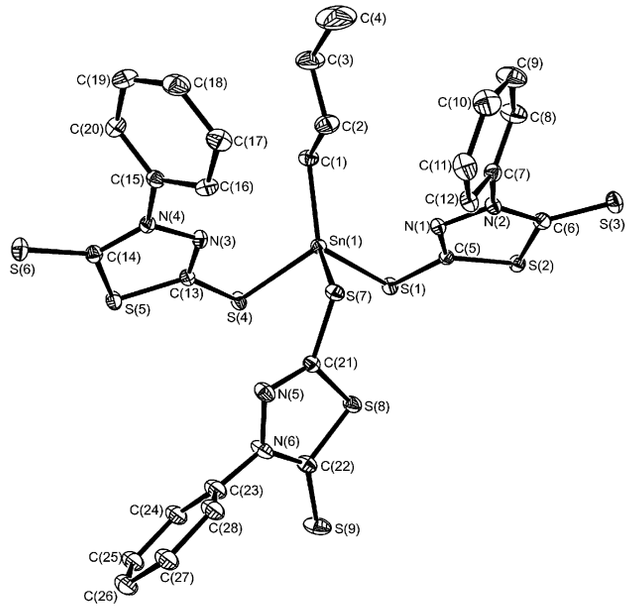

Fig. 1 The structure of compound **1**, showing the labelling used in the text. Thermal ellipsoids are at the 30% probability level (as in all figures). Selected metric data: Sn(1)–C(1) 2.128(3), Sn(1)–S(1) 2.4687(7), Sn(1)–S(4) 2.4616(6), Sn(1)–S(7) 2.4523(7), S(1)–C(5) 1.740(2), S(2)–C(5) 1.733(2), S(2)–C(6) 1.749(3), S(3)–C(6) 1.655(3), S(4)–C(13) 1.744(3), S(5)–C(13) 1.737(3), S(5)–C(14) 1.749(3), S(6)–C(14) 1.653(3), S(7)–C(21) 1.739(3), S(8)–C(21) 1.740(3), S(8)–C(22) 1.734(3), S(9)–C(22) 1.654(3), N(1)–C(5) 1.295(3), N(3)–C(13) 1.292(3), N(5)–C(21) 1.294(3) Å; C(1)–Sn(1)–S(1) 118.59(8), C(1)–Sn(1)–S(4) 117.41(8), C(1)–Sn(1)–S(7) 115.40(7), S(4)–Sn(1)–S(1) 95.83(2), S(7)–Sn(1)–S(1) 105.75(2), S(7)–Sn(1)–S(4) 100.81(2)°.

Since the intramolecular Sn ··· N interactions previously described are significantly longer than the intermolecular N⟶Sn secondary coordinations found for related compounds such as organotin tetrazoles [2.27(1)–2.43(1) Å],[21,22] the coordination pattern of the $PhN_2C_2S_3$ ligand can be described as essentially S-monodentate, with a weak chelation through the ring nitrogen, *i.e.* anisobidentate. The exocyclic C–S distances [C–S: 1.739(3)–1.744(3); C=S: 1.653(3)–1.655(3) Å] are close to the corresponding values found for coordinated thiol groups [1.70(1)–1.744(8) Å] and non-bonded thione groups [1.67(1) Å] in $C_3N_3S_3(SnR_3)_3$[5] and $[(C_3N_3S_3H)\{Co(en)_2\}_2]$-$[ClO_4]_3\cdot 2H_2O$.[23] Despite the weak chelation of two $PhN_2C_2S_3$ ligands, the C=N distances of all heterocycles are equal within experimental error [1.292(3)–1.295(3) Å] and are comparable to analogous bonds found in related aromatic heterocycles [*cf.* $[(C_3N_3S_3H)\{Co(en)_2\}_2][ClO_4]_3\cdot 2H_2O$, C=N: 1.33(2) Å].[23] The heterocyclic units are essentially planar [maximum deviation 0.016 Å] and the phenyl rings are twisted by *ca.* 50° [N–N–C–C: −49.7(3) to 57.7(3)°] with respect to these planes. As the structure of the $PhN_2C_2S_3$ ligand in **2**–**3**, **7** and **8** is similar to that found in **1**, it will be not discussed further.

Compound 2. The asymmetric unit of **2** was found to consist of one half of the molecule, the remainder being generated by a two-fold axis through the metal in the S–Sn–S′ plane and bisecting the C–Sn–C′ angle (Fig. 2). The Sn–S bond [2.470(2) Å] is typical and compares well with the analogous bonds in **1** [2.4523(7)–2.4687(7) Å] and related compounds [*cf.* $(PhN_4CS)_2SnBu_2$, Sn–S: 2.477(4) Å].[8] The coordination about tin is essentially tetrahedral, with two weak intramolecular Sn ··· N interactions [Sn(1) ··· N(1): 2.97 Å] distorting the coordination geometry towards an $C_2SnS_2N_2$ bicapped tetrahedron. This interaction is even weaker than those found for **1** [Sn ··· N: 2.773(2)–2.891(2) Å] and the C–Sn–S bond angles [109.8(2)–113.8(2)°] are closer to the ideal tetrahedral value. However, the distortion of the C–Sn–C′ [117.7(4)°] and S–Sn–S′ angles [88.35(9)°] reflects the weak anisobidentate chelation

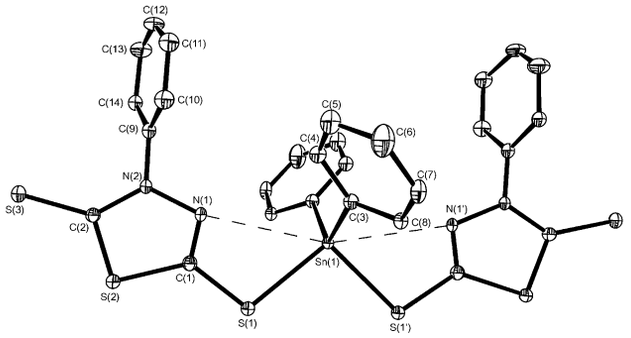

Fig. 2 The structure of compound **2**, showing the labelling used in the text. Selected metric data: Sn(1)–C(3) 2.117(7), Sn(1)–S(1) 2.470(2), S(1)–C(1) 1.748(8), S(2)–C(1) 1.727(7), S(2)–C(2) 1.751(8), S(3)–C(2) 1.666(7), N(1)–C(1) 1.278(10) Å; C(3)–Sn(1)–C(3′) 117.7(4), S(1)–Sn(1)–S(1′) 88.35(9), C(3)–Sn(1)–S(1) 113.8(2), C(3)–Sn(1)–S(1′) 109.8(2)°.

of the ligands, the latter value being comparable to the S–Sn–S′ value found for compounds displaying similar structural features [*cf.* $(PhN_4CS)_2SnBu_2$: 86.6(2); $Me_2Sn[S(O)CNC_4H_4]_2$: 92.6(1)°].[8,24]

Compound 3. The overall crystal structure of **3** (Fig. 3) contains two molecules (labelled as **A** and **B**) containing slightly different tin centres, as suggested by the Mössbauer spectroscopy. † The asymmetric unit of **3** was found to consist of two halves of each of molecules **A** and **B**, the remainder being generated by mirror planes bisecting the S–Sn–S planes and containing the α- and γ-carbon atoms of one Bu, as well as all the carbon atoms of the other Bu group. The molecular structure of **3** is similar to those of **2** and $Bu_2Sn(SCN_4Ph)_2$.[7] Thus, the heterocyclic ligands are primarily monodentate through their thiol (C–S) groups and the approximately equal Sn–S distances [**A**: 2.4832(7); **B**: 2.4894(8) Å] fall close to the corresponding bond lengths found for **2** [2.471(2) Å] and $Bu_2Sn(SCN_4Ph)_2$ [2.477(4) Å]. The coordination polyhedra at the tin atoms can be described as distorted tetrahedra or, alternatively, highly distorted octahedra. In accord with this view are the large C–Sn–C angles [**A**: 126.1(2); **B**: 136.7(2)°] and a concomitant decrease in the S–Sn–S angle [**A**: 88.86(4); **B**: 89.91(4)°]. When compared to related compounds, the C–Sn–C angles of **3** were found to be larger than that of **2** [117.7(4)°], the average of 131.4(2)° approximating the C–Sn–C angle of $Bu_2Sn(SCN_4Ph)_2$ [130.7(4)°]. Moreover, the acute S–Sn–S angles of **3** are comparable to the corresponding bond angles found for **2** [88.35(9)°] and $Bu_2Sn(SCN_4Ph)_2$ [86.6(2)°], falling close to the octahedral value of 90°. Nevertheless, the S–Sn–C angles of **3** lie in a narrow range [**A**: 107.26(8)–110.49(8); **B**: 104.55(8)–105.70(8)°] close to the tetrahedral value. These findings are in good agreement with an increase in the coordination number at the tin atom due to the weak anisobidentate chelation of the ligands through their ring nitrogen atoms. The intramolecular Sn ··· N interactions in **3** [**A**: 2.923(2); **B**: 2.911(2) Å] are comparable to those found for **2** [2.97 Å] and $Bu_2Sn(SCN_4Ph)_2$ (2.99 Å) and support the previous interpretation.

Compound 7. The molecular structure of **7** (Fig. 4) contains a trigonal bipyramidal *trans*-S_2SnC_3 centre, consistent with the spectral data. † All S–Sn–S and C–Sn–C bond angles [172.95(2) and 114.7(2)–119.3(1)°, respectively] support this description. The tin atom is directly bonded to the thiol (C–S) group of **I** and is further coordinated intermolecularly by the thione group (C=S) of a neighbouring molecule. The two Sn–S bonds are of different lengths. Thus, the Sn(1)–S(1) distance [2.5409(9) Å], although slightly longer than the corresponding bonds of **1**–**3** [Sn–S: 2.4523(7)–2.4894(8) Å], is comparable with the Sn–S bond lengths found for organotin thiotetrazoles [2.477(4)–2.614(5) Å].[4,7] Furthermore, the intermolecular Sn(1)–S(3) distance [3.2274(8) Å], though long, falls in the range proposed for secondary Sn ··· S coordination [2.79–3.81 Å][6] and the ligand can be described as unsymmetrical S(1),S(3)-bidentate bridging. Such coordination behaviour brings no major changes in the structure of the $PhN_2C_2S_3$ ligand, both C–S bond lengths [S(1)–C(4): 1.730(3) and S(3)–C(5): 1.668(3) Å] lying close to the corresponding distances found for **1**–**3** [C–S: 1.732(3)–1.748(8) and C=S: 1.653(3)–1.668(7) Å].

Compound 8. The asymmetric unit of **8** (Fig. 5) was found to consist of one half of the dinuclear molecule, the remainder being generated by an inversion centre at the midpoint of the 4,4′-bipy ligand. The structure contains two $Me_3Sn(S_3C_2N_2Ph)$ units associated through a bridging 4,4′-bipy moiety. The coordination environment around tin is *trans*-$NSSnC_3$ with the axial positions occupied by the thiol sulfur of the heterocycle and the ring nitrogen of the neutral bipyridyl donor. The S–Sn–

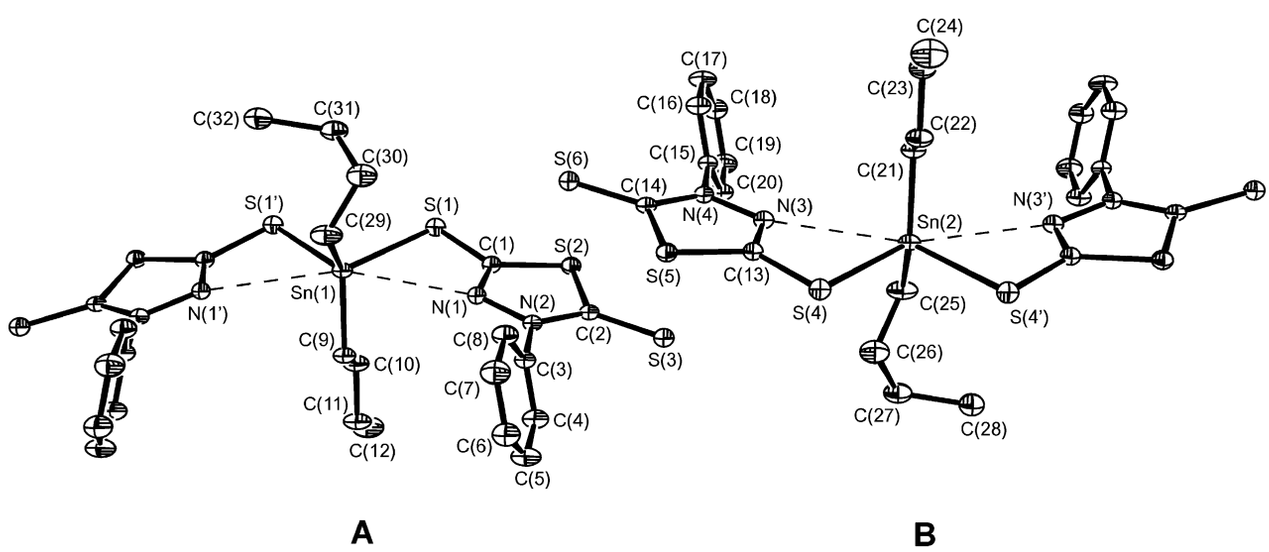

Fig. 3 The structure of compound **3**, showing the labelling used in the text. Selected metric data: Sn(1)–C(9) 2.128(4), Sn(1)–C(29) 2.133(5), Sn(1)–S(1) 2.4832(7), S(1)–C(1) 1.737(3), S(2)–C(1) 1.731(3), S(2)–C(2) 1.751(3), S(3)–C(2) 1.661(3), N(1)–C(1) 1.298(4), Sn(2)–C(21) 2.138(4), Sn(2)–C(25) 2.116(5), Sn(2)–S(4) 2.4894(8), S(4)–C(13) 1.732(3), S(5)–C(13) 1.732(3), S(5)–C(14) 1.746(3), S(6)–C(14) 1.660(3), N(3)–C(13) 1.303(4) Å; C(9)–Sn(1)–C(29) 126.10(16), S(1)–Sn(1)–S(1′) 88.86(4), C(9)–Sn(1)–S(1) 107.26(8), C(29)–Sn(1)–S(1) 110.49(8), C(25)–Sn(2)–C(21) 136.73(16), S(4)–Sn(2)–S(4′) 89.91(4), C(21)–Sn(2)–S(4) 105.70(8), C(25)–Sn(2)–S(4) 104.55(8)°.

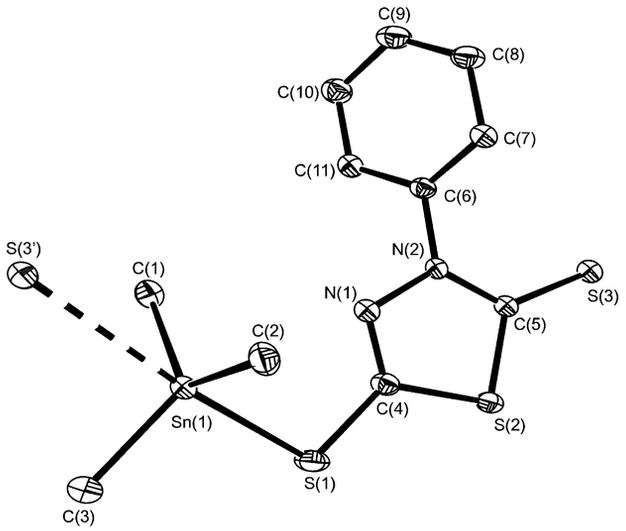

Fig. 4 The structure of compound **7**, showing the labelling used in the text. Selected metric data: Sn(1)–C(1) 2.132(3), Sn(1)–C(2) 2.130(3), Sn(1)–C(3) 2.134(3), Sn(1)–S(1) 2.5409(9), Sn(1)–S(3) 3.2274(8), S(1)–C(4) 1.730(3), S(2)–C(4) 1.748(3), S(2)–C(5) 1.739(3), S(3)–C(5) 1.668(3), N(1)–C(4) 1.296(4) Å; C(2)–Sn(1)–C(1) 119.28(14), C(2)–Sn(1)–C(3) 118.73(16), C(1)–Sn(1)–C(3) 114.68(16), C(1)–Sn(1)–S(1) 104.92(10), C(2)–Sn(1)–S(1) 97.24(11), C(3)–Sn(1)–S(1) 95.01(10), C(1)–Sn(1)–S(3) 77.56(8), C(2)–Sn(1)–S(3) 75.90(9), C(3)–Sn(1)–S(3) 89.82(9), S(1)–Sn(1)–S(3) 172.95(2)°.

N [176.27(4)°] and C–Sn–C angles [118.5(1)–126.6(1)°] reflect this coordination geometry. The Sn–S bond length [2.6174(7) Å] is slightly longer when compared with that of **7** [2.5409(9) Å] and is at the longer end of the range of Sn–S distances measured for organotin thiotetrazoles [2.477(4)–2.614(5) Å].[4,7] Furthermore, the Sn–N bond [2.613(2) Å] is longer than those found in organotin tetrazoles [2.27(1)–2.43(1) Å][21,22] or the cationic polymer $[Me_3Sn(4,4'\text{-bipy})]_n^{n+}$ [2.411(2), 2.420(2) Å].[25,35]

Compound 9. The molecular structure of **9** (Fig. 6) reveals the presence of two non-associated ionic units, a $[Me_3Sn(PyNH_2\text{-}4)_2]^+$ cation and a $[PhN_2C_2S_3]^-$ anion. The cationic unit contains a *trans*-trigonal bipyramidal tin centre, as found in **7** and **8**, although in **9** this geometry is obtained by coordination of the ring nitrogen atoms of two neutral $PyNH_2$-4 donors, which complete the coordination sphere about tin. The two Sn–N distances [2.358(2), 2.351(2) Å] are equal within experimental error and are somewhat shorter than those found in the polymeric cation $[Me_3Sn(4,4'\text{-bipy})]_n^{n+}$ [2.411(2), 2.420(2) Å].[25] The cationic nature of the tin in **9** clearly has enhanced Lewis acidity, hence the increased strength of the bonds to the coordinated pyridine donors. Similar to **7** and **8**, the axial and equatorial bond angles in **9** are close to the ideal values expected for a trigonal bipyramidal environment around tin.

The non-bonded anionic heterocyclic ligand is situated in the vicinity of the $-NH_2$ groups of both coordinated $PyNH_2$-4 molecules, with N–H ··· S hydrogen bonds between the amino groups and the exocyclic S atoms being evident (see below). The differences between the structure of the $PhN_2C_2S_3^-$ anion in **9** and the related ligands in **1**–**3**, **7** and **8** derive from the lengths of C–S and C=S bonds. Thus, the shortening of the thiol bond [C(1)–S(1): 1.705(2); *cf.* 1.725(2)–1.748(8) Å in **1**–**3**, **7** and **8**] is probably due to the lack of any S–Sn interaction, while the marginal lengthening of the thione bond [C(2)–S(3): 1.683(2) *vs.* 1.653(3)–1.668(3) Å in **1**–**3**, **7** and **8**] probably reflects the relative strength of the H-bond in **9** compared to weak bridging in **7** and no –or much weaker– secondary interactions in **1**–**3** and **8**.

Supramolecular structures

The supramolecular structure of **1** is complex, as a large number of intermolecular S ··· S contacts are apparent. Notably however, the thiol sulfurs S(1) and S(4), which approach each other most closely intramolecularly [<S–Sn–S: 95.83(2)°], have no intermolecular contacts < 3.7Å. Conversely, thiol S(7) and endocyclic S(2) are 3.59 Å from each other, while the remaining endocyclic sulfurs partner thiones [S(5) ··· S(9): 3.34, S(3) ··· S(8): 3.49 Å], leaving thione S(6) largely uninvolved [S(6) ··· S(1): 3.78 Å].

The supramolecular structures of **3**, **7**, **8** and **9** are dominated by molecular chains propagated through S⟶Sn and/or S ··· S and/or N–H ··· S intermolecular interactions. The molecules of **3** aggregate in the solid state through weak intermolecular S ··· S interactions [S(2) ··· S(6): 3.710(1); S(3) ··· S(5): 3.817(1) Å] directed by the endocyclic and thione sulfur atoms of each pair of neighbouring ligands (Fig. 7). The two S ··· S interactions describe a six-membered ring (S_4C_2) which deviates significantly from planarity [torsion angle C(2)–S(3)–S(5)–C(14): −53.8(1)°] in a characteristic 'chair' conformation. Despite these S ··· S distances being at the limit of a Van der Waals interaction (3.8 Å, based on recent data derived from Me_2S),[26] they clearly govern the self-assembly of the molecules into monodimensional chains which run parallel to each other along the *a* axis.

As with **1**, the thiol sulfurs which show close approach intramolecularly [<S–Sn–S 88.86(4), 89.91(4)°], are not involved in intermolecular contacts. The same situation also pertains in **2**, though somewhat surprisingly the endocyclic and thione

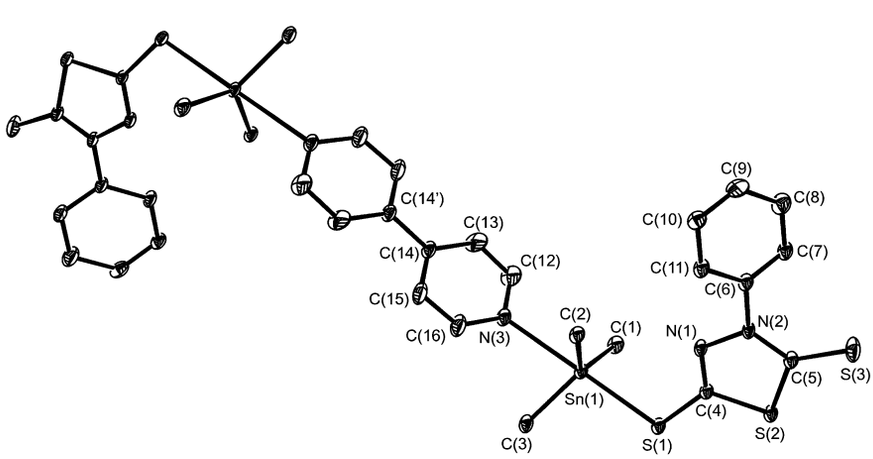

Fig. 5 The structure of compound **8**, showing the labelling used in the text. Selected metric data: Sn(1)–C(1) 2.126(3), Sn(1)–C(2) 2.128(2), Sn(1)–C(3) 2.136(2), Sn(1)–S(1) 2.6174(7), S(1)–C(4) 1.725(2), S(2)–C(4) 1.753(2), S(2)–C(5) 1.747(3), S(3)–C(5) 1.661(3), N(1)–C(4) 1.298(3) Å; C(1)–Sn(1)–C(2) 122.82(11), C(1)–Sn(1)–C(3) 118.54(11), C(2)–Sn(1)–C(3) 115.59(10), C(1)–Sn(1)–S(1) 95.31(8), C(2)–Sn(1)–S(1) 98.51(7), C(3)–Sn(1)–S(1) 93.52(7), C(1)–Sn(1)–N(3) 88.04(6), C(2)–Sn(1)–N(3) 78.26(6), C(3)–Sn(1)–N(3) 86.29(6), S(1)–Sn(1)–N(3) 176.28(4)°.

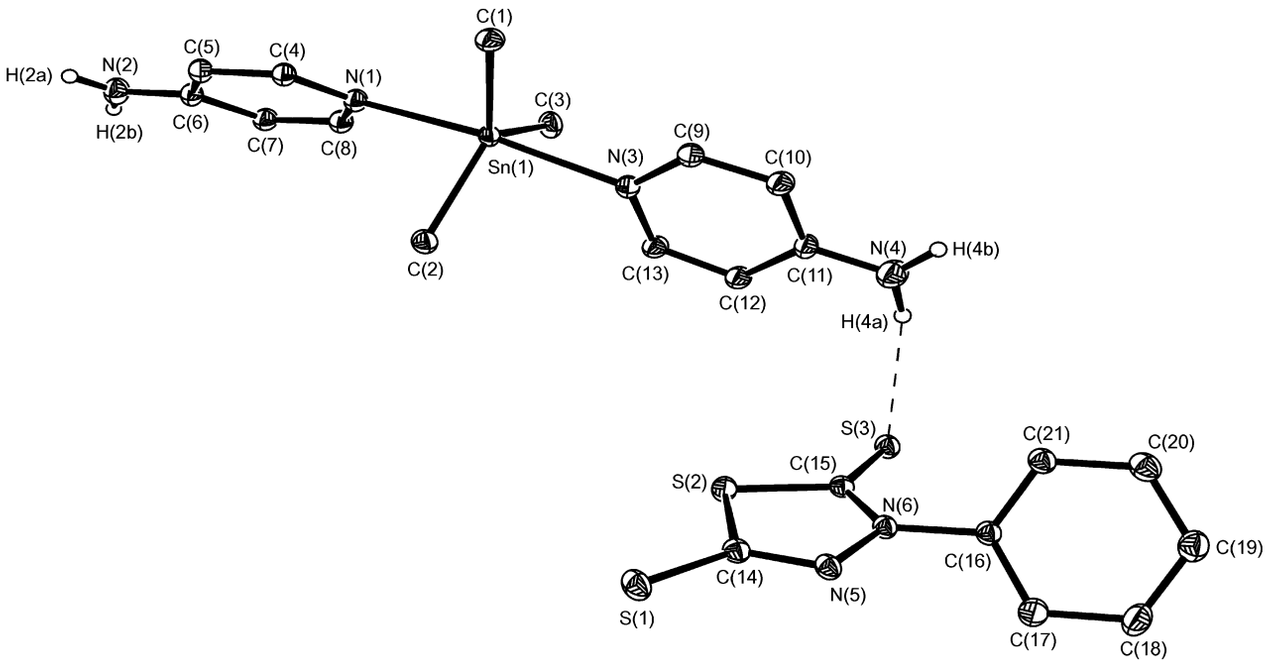

Fig. 6 The structure of compound **9**, showing the labelling used in the text. Selected metric data: Sn(1)–C(1) 2.126(3), Sn(1)–C(2) 2.132(2), Sn(1)–C(3) 2.127(2), Sn(1)–N(1) 2.358(2), Sn(1)–N(3) 2.351(2), S(1)–C(14) 1.705(2), S(2)–C(14) 1.765(2), S(2)–C(15) 1.733(2), S(3)–C(15) 1.683(2), N(5)–C(14) 1.305(3) Å; C(1)–Sn(1)–C(3) 120.44(10), C(1)–Sn(1)–C(2) 119.09(10), C(2)–Sn(1)–C(3) 120.46(10), C(1)–Sn(1)–N(1) 94.08(8), C(2)–Sn(1)–N(1) 86.21(8), C(3)–Sn(1)–N(1) 90.79(8), C(1)–Sn(1)–N(3) 93.06(8), C(2)–Sn(1)–N(3) 89.71(8), C(3)–Sn(1)–N(3) 86.20(8), N(1)–Sn(1)–N(3) 172.83(7)°.

sulfurs of **2** show no short contacts, which contrasts markedly with **3**.

The intermolecular C=S⟶Sn coordination in **7** leads to infinite polymer chains containing the metal centres and heterocyclic groups in approximately the same plane [torsion angle N(1)–C(4)–S(1)–Sn(1): −14.8(3); Sn(1)–S(3)–C(2)–S(2): 19.7(5)°]. Relative to each chain, a second chain runs parallel, inverted with respect to the first and linked by weak S ⋯ S interactions [S(1) ⋯ S(2′) 3.689(2) Å] directed by the endocyclic and the thiol sulfur atoms [Fig. 8(a)], which are slightly shorter than those found for **3**. Similar to **3**, the two S ⋯ S linkages take place between each pair of neighbouring ligands and generate a six-membered ring (S_4C_2) which displays a less acute 'chair' conformation [torsion angle C(4)–S(1)–S(2′)–C(4′): −30.5(2)°]. These interactions connect the polymers in 'ribbon'-type double-chain arrays. Furthermore, the thiol sulfurs S(1) of the neighbouring double-chain ribbons interconnect at a distance of 3.675(1) Å and the Ph groups which occupy the space between these ribbons π-stack in a face-to-face manner [Ph ⋯ Ph: 3.53–3.56 Å] [Fig. 8(b)]. This structural feature leads to an expansion of the supramolecular structure of **7** to a three-dimensional network.

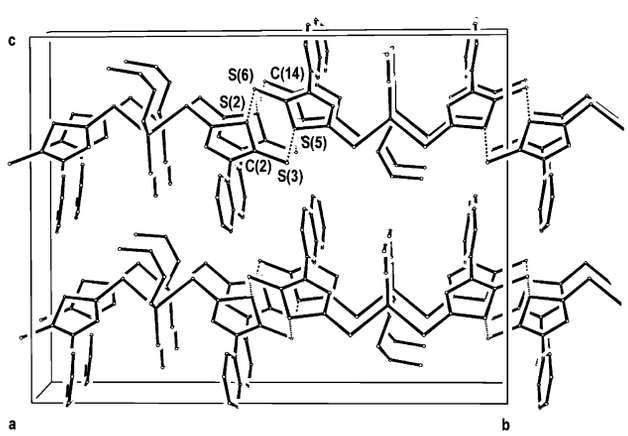

Fig. 7 The supramolecular structure of **3**, showing weak intermolecular S ⋯ S interactions

The molecules of **8** also aggregate in the solid state through intermolecular S ⋯ S interactions, generating monodimensional chains that run parallel to each other (Fig. 9). When compared to the supramolecular structure of **3** and **7**, only the coordinated thiol sulfurs in **8** are involved in such contacts, probably due to the large size and rigidity of the dinuclear molecules. On the other hand, the S ⋯ S distance in **8** [S(1) ⋯ S(1′): 3.4561(7) Å] is significantly shorter than those found for **3** [3.710(1)–3.817(1) Å] and **7** [3.675(1)–3.689(2) Å] and compares favourably to similar S ⋯ S interactions found for molecular superconductors, such as donor–acceptor compexes of bis(ethylenedithio)tetrathiafulvalene (3.3–3.6 Å).[20] As no further intermolecular interactions were identified in the crystal structure of **8**, the supramolecular structure can be described as essentially 1-D.

The supramolecular structure of **9** consists of a three-dimensional network in which $[Me_3Sn(PyNH_2\text{-}4)_2]^+$ cations and $[PhN_2C_2S_3]^-$ anions are self-assembled by N–H ⋯ S hydrogen bonding, generated by the NH_2 groups of both 4-H_2NPy molecules coordinated to tin and the neighbouring thiol S(1) and thione S(3) sulfurs of the anionic heterocycle (Fig. 10). It is noteworthy that the involvement of the non-bonded anionic ligand (at least as far as the metal is concerned) in the construction of the supramolecular structure is unprecedented when compared to previously characterised fully ionic compounds containing an $[R_3SnD_2]^+$ cation (D = H_2O, CH_3CN, NH_3 and 0.5 4,4′-bipy).[25,27–29] The N(2)–H(2B) ⋯ S(1) [N(2) ⋯ S(1): 3.562, H(2B) ⋯ S(1): 2.665 Å; N(2)–H(2B) ⋯ S(1): 175.22°] and N(4)–H(4B) ⋯ S(3) linkages [N(4) ⋯ S(3): 3.365, H(4B) ⋯ S(3): 2.521 Å; N(4)–H(4B) ⋯ S(3): 159.54°] lead to molecular chains, containing alternating $[Me_3Sn(PyNH_2\text{-}4)_2]^+$ cations and $[PhN_2C_2S_3]^-$ anions, which run parallel to each other along the *a* axis. Furthermore, these chains interconnect through N(2)–H(2A) ⋯ S(1) [N(2) ⋯ S(1): 3.541, H(2A) ⋯ S(1): 2.693 Å; N(2)–H(2A) ⋯ S(1): 161.31°] and N(4)–H(4A) ⋯ S(3) interactions [N(4) ⋯ S(3): 3.392, H(4A) ⋯ S(3): 2.559 Å; N(2)–H(4A) ⋯ S(3): 161.66°], resulting in an expanded 3-D network. There are very few examples of designed supramolecular assemblages of sulfur-mediated hydrogen bonds. Recent crystallographic studies of trithio-

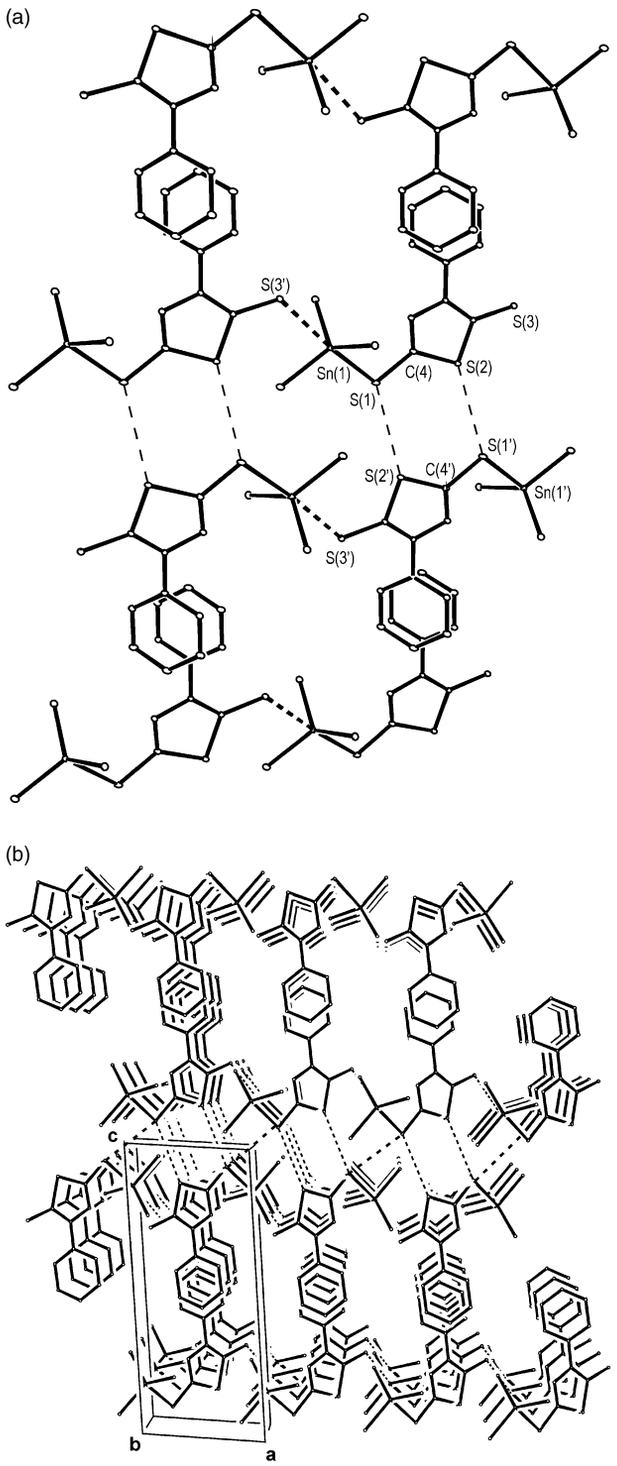

Fig. 8 The supramolecular structure of **7**, showing (a) polymer propagation *via* S⟶Sn coordination and interchain S ··· S contacts and (b) additional inter-ribbon S ··· S contacts and π-stacking of aromatic groups.

cyanuric acid and its adducts with Me_2CO, melamine and 4,4′-bipy revealed layer- and chanel-type supramolecular architectures built up *via* intermolecular N–H ··· S interactions [H ··· S: 2.32–2.56 Å].[30,31] Although the hydrogen bonds in **9** are weaker than those previously described, they govern the assembly of the molecules in the three dimensional architecture. Moreover, the formation of hydrogen bonds involving sulfur atoms is at the expense of weaker S ··· S interactions, which are absent in this structure.

Conclusions

The most significant conclusions that can be drawn from this study relate to the roles of intermolecular coordination, hydrogen bonding and S ··· S interactions in controlling supramolecular assemblies. Although this work relates specifically to organotin chemistry, some potentially more general inferences can be drawn.

Firstly, only the thione sulfur involves itself in intermolecular coordination to tin. Bridging sulfur ligands are rare in organotin chemistry, particularly in comparison with the plethora of N- and O-bridged structures. In cases where N-donors are available (**8**, **9**), these preferentially coordinate the metal at the expense of C=S⟶Sn. That such an interaction is observed in the trimethyltin compound **7**, but not in any of the di- and mono-organotin analogues **1**–**3**, probably reflects the preference of the softer triorganotin monocation for sulfur, the $[R_{4-n}Sn]^{n+}$ ($n = 2, 3$) receptors opting for weak internal chelation by harder N-donors. Interestingly, the structure of $Me_3Sn[SP(Ph)_2NP(Ph)_2S]$, which we have previously determined, is the only other structurally authenticated 1-D, S-bridged organotin polymer[32] and provides the only instance of a dithioimidodiphosphinate ligand behaving this way.

Where metal coordination does not occur, the thione group chooses a hydrogen-bonding role rather than involvement in S ··· S interactions (**9**), and only when neither of the first two options are available do the latter occur (**1**–**3**, **8**). Additionally, hydrogen bonds are also formed by the thiol sulfur in preference to S ··· S interactions (**9**), but are slightly weaker than those involving the thione group (**9**: 3.37, 3.39 *vs* 3.54, 3.56 Å).

The pattern of S ··· S interactions in the compounds studied in this work is complex, but a general trend appears to be emerging which largely rationalises the sequence in which thiol, thione and endocyclic sulfur centres involve themselves in such an array. Homoleptic thiol–thiol interactions seem to be the most significant, since in **8** (where S⟶Sn and H-bonding are absent), all the sulfurs are available, yet only (thiol)S ··· S(thiol) contacts are observed, and these are relatively short (3.46 Å). In **1**–**3**, we believe that the absence of significant intermolecular (thiol)S ··· S(thiol) contacts arises because analogous *intramolecular* interactions are already present. Three pieces of evidence support this claim: firstly, acute S–Sn–S angles are observed, which are not required by the overall molecular geometry and/or coordination number at tin; secondly, we have noted similar angular deformations in $(RS)_4Sn$ and which subsequently lead to thermal elimination of RSSR in CVD experiments;[1] finally, in **1**, the only notable intermolecular contact involving a thiol sulfur occurs with that thiol *not* involved in the close intramolecular S ··· S interaction [S(2)–S(7) 3.59 Å].

Homoleptic S ··· S contacts between pairs of either thione or endocyclic sulfurs do not occur, but both thiol–endocyclic and thione–endocyclic pairings are observed. The available data do not yet allow discrimination between the strengths of these contacts. For example, comparison of **3** and **7** suggests that (thione)S ··· S(endo) contacts are marginally weaker (**3**: > 3.7 Å) than (thiol)S ··· S(endo) interactions (**7**: *ca.* 3.7 Å), but in **1**, the (thione)S ··· S(endo) interactions are notably stronger (3.34, 3.49 Å) and are shorter than the one (thiol)S ··· S(endo) contact (**1**: 3.59 Å).

We have made some attempt to rationalise these findings with the aid of density functional theory to model the charge distribution in the $PhN_2C_2S_3$ ligand (L) and related species (Table 1), though, clearly, any approach which deals with isolated molecules cannot fully account for species in which intermolecular interactions are widespread.

In each of the modelled species, L^-, LH and $LSnMe_3$, the lowest energy arrangement has the exocyclic phenyl group twisted with respect to the heterocycle, by angles of 29.7, 44.4 and 50.8°, respectively, though the potential energy surface for twist angles of 0–90° is rather flat. These values compare well with twist angles of 47.9–66.3° observed across the six structure determinations in this paper. The key internuclear distances in

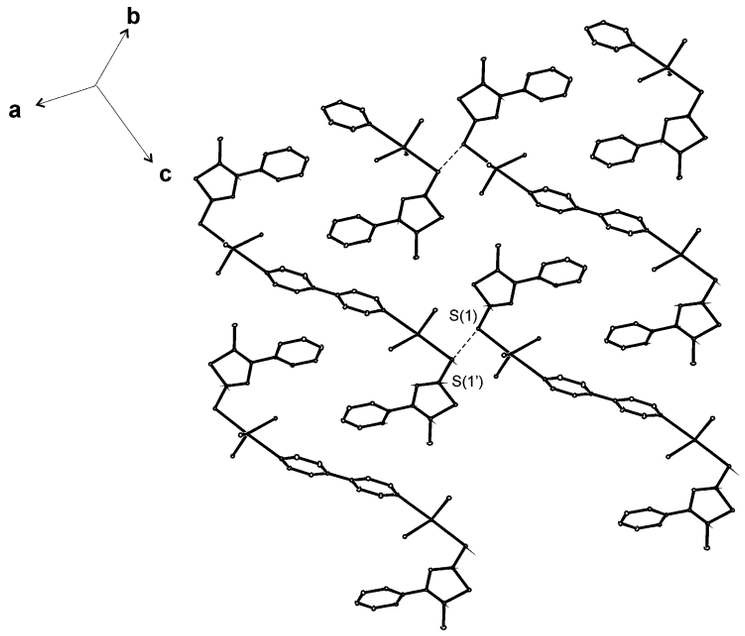

Fig. 9 The supramolecular structure of **8**, showing intermolecular S ··· S interactions

Table 1 Calculated bond lengths and atomic charges for L and related species

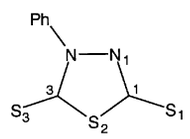

(L)

	Bond lengths/Å					Atomic charges		
	S_1–C_1	S_2–C_1	S_2–C_3	S_3–C_3	N_1–C_1	S_1	S_2	S_3
L^-	1.698	1.812	1.755	1.689	1.316	−0.36	+0.38	−0.28
9	1.705	1.765	1.733	1.683	1.305			
LH	1.765	1.755	1.787	1.653	1.291	+0.09	+0.45	−0.10
$LSnMe_3$	1.754	1.762	1.781	1.656	1.297	−0.21	+0.46	−0.12
8	1.725	1.753	1.744	1.661	1.298			

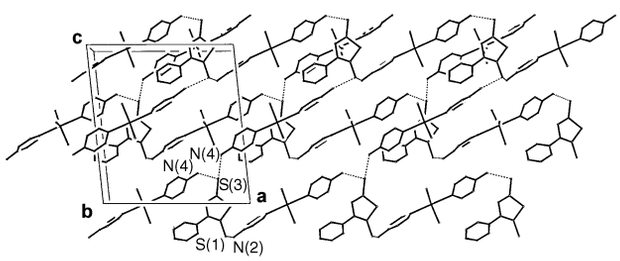

Fig. 10 The supramolecular structure of **9**, showing self-assembly through N–H ··· S hydrogen bonds.

the anion are modelled rather well, though the S_2–C_1 and S_2–C_3 separations within the heterocycle are calculated to be slightly longer than found in **9**. A similar comment can be made about the analogous distances calculated for an isolated molecule of $LSnMe_3$ (tetrahedral tin), where the S_2–C_1 and S_2–C_3 bonds are predicted to be longer than found in **8**. In addition, for both LH and $LSnMe_3$, the two S–C bonds within the heterocycle are predicted to be reversed in order of bond length compared to the anion L^-, which is not clearly observed in the structures of **1**–**3**, **7** and **8**. However, in all of these latter structures the two endocyclic S–C bonds are equal within experimental error and in **1** (two out of three heterocycles), **2** and **3** the predicted ordering (before considering esds) is observed.

In the models of L^- and $LSnMe_3$, the exocyclic sulfurs are predicted to both bear negative charges, while the endocyclic sulfur is predicted to be positive in both cases. This rationalises the pairing of the endocyclic sulfur with either of the exocyclic centres in intermolecular S ··· S formation, *i.e.* it is charge controlled. It also explains why only the (negative) exocyclic sulfurs engage in the hydrogen bonding observed in **9**.

What is less easy to accommodate is the formation of S ··· S interactions solely involving S_1. Homoatomic S ··· S interactions will always bring together two atoms of identical charge, so it is perhaps not surprising that S_2 (repulsion of +/+) and S_3 (repulsion of −/−) do not form close homoatomic contacts. On the other hand, S_1 ··· S_1 contacts are observed in both **7** and **8**, and we can only speculate that this is perhaps due to the polarisability of this sulfur. In our models, in contrast to S_2 and S_3, which maintain a common net charge in L^-, LH and $LSnMe_3$, the net charge on S_1 varies from −0.36 to +0.09 to −0.21 across the same series (Table 1). However, there seems no obvious reason from these data why the formation of polarisation-induced homoatomic S_1 ··· S_1 interactions should occur in preference to charge-matched S_1–S_2 or S_3–S_2 interactions, as seen in **8**.

Experimental

Spectra were recorded on the following instruments: JEOL GX270, Bruker AC270, JEOL GX400, Bruker AC400 (^{1}H, ^{13}C and ^{119}Sn NMR), Perkin-Elmer 599B (IR). The NMR spectra were recorded in saturated $CDCl_3$ (**1**–**8**) or $(CD_3)_2SO$ (**I**, **9**) solutions at room temperature. For all compounds, IR spectra

were recorded in Nujol mulls. Details of the Mössbauer spectrometer and related procedures are given elsewhere.[33] Isomer shift data are relative to $CaSnO_3$ at 78 K. All other chemicals were obtained commercially (*e.g.* Aldrich) and used without further purification. All preparations were conducted under an inert atmosphere using dried solvents.

Syntheses

5-Mercapto-3-phenyl-1,3,4-thiadiazoline-2-thione potassium salt, monohydrate (I). The synthesis of $PhN_2C_2S_3K\cdot H_2O$ is a modification of the literature method.[34] $PhNHNH_2$ (5.4 g, 50 mmol) was dissolved in a mixture of *N*,*N*-dimethylformamide (50 ml) and pyridine (10 ml), and CS_2 (10 ml) was added dropwise. The reaction was warmed slowly to 100 °C over a period of 1–2 h and stirred at this temperature for 30 min, until H_2S evolution was complete. After removing the solvent *in vacuo*, the resulting waxy solid was re-dissolved in a mixture of water (100 ml) and aqueous 5% Na_2CO_3 solution (10 ml); the small amount of solid remaining was extracted in diethyl ether. The aqueous solution was separated, treated with concentrated HCl (7 ml) and the resulting precipitate filtered off and dried at room temperature to give the acid, $PhN_2C_2S_3H$, as a white powder (9.5 g, 84%).

$PhN_2C_2S_3H$ (9.5 g, 42 mmol) was re-dissolved in hot EtOH (100 ml). The addition of an EtOH solution (100 ml) of KOH (2.4 g, 42 mmol) induced precipitation of the product as a microcrystalline white solid (10.5 g, 89%), mp 236 °C. Found (calc. for $C_8H_7N_2OS_3K$): C, 33.7 (34.0); H, 2.5 (2.5); N 9.9 (9.8)%. ^{1}H NMR: δ 7.67 (d, 2H, 2-Ph, ^3J 7.5), 7.46 (dd, 2H, 3-Ph, ^3J 7.2/8.1), 7.36 (dd, 1H, 4-Ph, ^3J 7.2/7.5 Hz), 3.59 (s, 2H, H_2O). ^{13}C NMR: δ 185.0 (C–S), 173.7 (C=S), 139.6 (1-Ph), 128.9 (3-Ph), 128.3 (4-Ph), 126.1 (2-Ph). IR (cm^{-1}): 3364, 1596, 1590, 1352, 1239, 1071, 1046, 830, 758, 696, 683.

Tris(5-mercapto-3-phenyl-1,3,4-thiadiazoline-2-thionato)-butyltin (1). I (0.96 g, 3.4 mmol) was suspended in a thf (50 ml) solution of $BuSnCl_3$ (0.28 g, 1.0 mmol) and the mixture was stirred overnight at room temperature. After removing the solid residue and concentrating the filtrate to low volume, the addition of hexane (50 ml) induced crystallisation of the product as a microcrystalline yellow solid (0.65 g, 77%), mp 128 °C dec. Found (calc. for $C_{28}H_{24}N_6S_9Sn$): C, 39.4 (39.5); H, 2.9 (2.8); N 9.6 (9.9)%. ^{1}H NMR: δ 7.53 (d, 6H, 2-Ph; ^3J 7.0), 7.43 (m, 9H, 3,4-Ph), 2.07 [m, 2H, $SnCH_2(CH_2)_2CH_3$], 1.27 (m, 2H, $SnCH_2CH_2CH_2CH_3$), 0.89 [m, 2H, $Sn(CH_2)_2CH_2CH_3$], 0.46 [t, 3H, $Sn(CH_2)_3CH_3$; ^3J 7.0 Hz]. ^{13}C NMR: δ 186.6 (C–S), 155.1 (C=S), 137.3 (1-Ph), 129.3 (3-Ph), 129.0 (4-Ph), 125.5 (2-Ph), 36.4 ($SnCH_2CH_2CH_2CH_3$), 27.5 [$SnCH_2(CH_2)_2CH_3$], 25.3 [$Sn(CH_2)_2CH_2CH_3$], 13.1 [$Sn(CH_2)_3CH_3$]. ^{119}Sn NMR: δ −10.2. Mössbauer (mm s^{-1}): i.s. 1.52; q.s. 1.93. IR (cm^{-1}): 1590, 1340, 1233, 1061, 827, 765, 710, 692, 681.

The complexes **2**–**7** were also prepared by the same method:

Bis(5-mercapto-3-phenyl-1,3,4-thiadiazoline-2-thionato)-diphenyltin (2). Yield 62%, mp 212 °C. Found (calc. for $C_{28}H_{20}N_4S_6Sn$): C, 46.4 (46.5); H, 2.8. (2.8); N, 7.8 (7.7)%. ^{1}H NMR: δ 7.76 (d, 4H, 2-PhSn; ^3J 6.6), 7.55 (d, 4H, 2-Ph; ^3J 8.2 Hz), 7.52–7.36 (m, 12H, 3,4-Ph, 3,4-PhSn)]. ^{13}C NMR: δ 185.4 (C–S), 138.6 (1-Ph), 135.8 (1-PhSn), 134.5 (3-PhSn), 128.5 (3-Ph), 128.3 (4-Ph), 128.25 (4-PhSn), 125.7 (2-Ph). ^{119}Sn NMR: δ −84.4. Mössbauer (mm s^{-1}): i.s. 1.36; q.s. 2.49. IR (cm^{-1}): 1587, 1342, 1244, 1056, 1019, 816, 766, 711, 687, 682.

Bis(5-mercapto-3-phenyl-1,3,4-thiadiazoline-2-thionato)-dibutyltin (3). Yield 73%, mp 118 °C. Found (calc. for $C_{24}H_{28}N_4S_6Sn$): C, 42.1 (42.2); H, 4.1 (4.1); N 8.0 (8.2)%. ^{1}H NMR: δ 7.57 (d, 4H, 2-Ph; ^3J 7.8), 7.46 (m, 6H, 3,4-Ph), 1.75 [m, 4H, $SnCH_2(CH_2)_2CH_3$], 1.46 (quint, 4H, $SnCH_2CH_2CH_2CH_3$; ^3J 7.8), 1.18 [sext, 4H, $Sn(CH_2)_2CH_2CH_3$; ^3J 7.2], 0.69 (t, 6H, $Sn(CH_2)_3CH_3$; ^3J 7.2 Hz]. ^{13}C NMR: δ 187.2 (C–S), 158.8 (C=S), 138.1 (1-Ph), 129.6 (3-Ph), 129.4 (4-Ph), 126.1 (2-Ph), 28.3 ($SnCH_2CH_2CH_2CH_3$), 26.7 [$SnCH_2(CH_2)_2CH_3$], 26.3 [$Sn(CH_2)_2CH_2CH_3$], 13.9 [$Sn(CH_2)_3CH_3$], ^1J[^{13}C–^{117,119}Sn] 447.0/468.1, ^2J[^{13}C–^{117,119}Sn] 32.39 Hz (unresolved). ^{119}Sn NMR: δ 58.9. Mössbauer (mm s^{-1}): i.s. 1.12, 1.42; q.s. 2.26, 2.85. IR (cm^{-1}): 1588, 1344, 1251, 1059, 1020, 826, 761, 707, 690.

Bis(5-mercapto-3-phenyl-1,3,4-thiadiazoline-2-thionato)-dimethyltin (4). Yield 76%, mp 142 °C. Found (calc. for $C_{18}H_{16}N_4S_6Sn$): C, 35.9 (36.1); H, 2.7 (2.7); N 9.3 (9.4)%. ^{1}H NMR: δ 7.62 (d, 4H, 2-Ph; ^3J 7.8 Hz), 7.46 (m, 6H, 3,4-Ph), 1.11 (s, 6H, $SnCH_3$), ^2J[^{1}H–^{117,119}Sn] 66.4 Hz (unresolved). ^{13}C NMR: δ 187.0 (C–S), 157.8 (C=S), 138.0 (1-Ph), 129.4 (3-Ph), 129.35 (4-Ph), 125.8 (2-Ph), 5.6 ($SnCH_3$), ^1J[^{13}C–^{117,119}Sn] 448.4/428.3 Hz. ^{119}Sn NMR: δ 71.3. Mössbauer (mm s^{-1}): i.s. 1.41; q.s. 2.67. IR (cm^{-1}): 1583, 1350, 1249, 1069, 1055, 828, 783, 759, 706, 684, 668.

(5-Mercapto-3-phenyl-1,3,4-thiadiazoline-2-thionato)triphenyltin (5). Yield 75%, mp 128 °C, Found (calc. for $C_{26}H_{20}N_2S_3Sn$): C, 54.3 (54.3); H, 3.5 (3.5); N 4.9 (4.9)%. ^{1}H NMR: δ 7.64 (d, 6H, 2-PhSn; ^3J 6.6 Hz), 7.45–7.24 (m, 14H, 3,4-PhSn, 2,3,4-Ph). ^{13}C NMR: δ 186.7 (C–S), 155.8 (C=S), 137.7 (1-Ph), 136.6 (1-PhSn), 136.3 (3-PhSn), 130.0 (3-Ph), 128.9 (4-Ph), 128.6 (4-PhSn), 128.4 (2-PhSn), 125.4 (2-Ph). ^{119}Sn NMR: δ −62.4. Mössbauer (mm s^{-1}): i.s. 1.34; q.s. 2.85. IR (cm^{-1}): 1590, 1356, 1237, 1073, 1031, 834, 762, 693, 682.

(5-Mercapto-3-phenyl-1,3,4-thiadiazoline-2-thionato)tributyltin (6). Pale yellow oil at room temperature, yield 72%, Found (calc. for $C_{20}H_{32}N_2S_3Sn$): C, 46.3 (46.4); H, 6.2 (6.3); N 5.4 (5.4)%. ^{1}H NMR: δ 7.68 (d, 2H, 2-Ph; ^3J 8.1), 7.44 (m, 3H, 3,4-Ph), 1.54 [m, 6H, $SnCH_2CH_2CH_2CH_3$], 1.29 (m, 12H, $SnCH_2CH_2CH_2CH_3$), 0.85 (dd, 9H, $Sn(CH_2)_3CH_3$; ^3J 7.1/7.5 Hz]. ^{13}C NMR: δ 187.2 (C–S), 158.2 (C=S), 138.4 (1-Ph), 128.7 (3,4-Ph), 125.5 (2-Ph), 28.3 ($SnCH_2CH_2CH_2CH_3$), 26.8 [$Sn(CH_2)_2CH_2CH_3$], 16.1 [$SnCH_2(CH_2)_2CH_3$], 13.4 [$Sn(CH_2)_3CH_3$], ^1J[^{13}C–^{117,119}Sn] 310.7/325.0, ^2J[^{13}C–^{117,119}Sn] 23.1 (unresolved), ^3J[^{13}C–^{117,119}Sn] 65.0 (unresolved). ^{119}Sn NMR: δ 120.5. Mössbauer (mm s^{-1}): i.s. 1.41; q.s. 2.75. IR (cm^{-1}): 1592, 1336, 1237, 1072, 1045, 822, 758, 701, 687, 668.

(5-Mercapto-3-phenyl-1,3,4-thiadiazoline-2-thionato)trimethyltin (7). Yield 81%, mp 96 °C. Found (calc. for $C_{11}H_{14}N_2S_3Sn$): C, 34.0 (34.0); H, 3.6 (3.6); N 7.1 (7.2)%. ^{1}H NMR: δ 7.70 (d, 2H, 2-Ph; ^3J 7.8), 7.47 (t, 2H, 3-Ph; ^3J 7.8 Hz), 7.40 (m, 1H, 4-Ph), 0.63 (s, 9H, $SnCH_3$), ^2J[^{1}H–^{117,119}Sn] 56.2 Hz (unresolved). ^{13}C NMR: δ 186.9 (C–S), 157.8 (C=S), 138.3 (1-Ph), 128.7 (3-Ph), 128.6 (4-Ph), 125.3 (2-Ph), −2.79 ($SnCH_3$), ^1J[^{13}C–^{117,119}Sn] 347.0/363.6 Hz. ^{119}Sn NMR: δ 126.1. Mössbauer (mm s^{-1}): i.s. 1.36; q.s. 2.89. IR (cm^{-1}): 1600, 1350, 1242, 1153, 1077, 1042, 830, 773, 760, 681, 667.

Bis-[(5-mercapto-3-phenyl-1,3,4-thiadiazoline-2-thionato)-trimethyltin]·4,4′-bipyridine (8). A large excess of 4,4′-bipy (0.31 g, 2.0 mmol) was added to a solution of **7** (0.39 g, 1.0 mmol) in diethyl ether (60 ml). After stirring for 3 h at room temperature, the colourless solution was concentrated and stored at low temperature to yield the product as a colourless crystalline solid (0.37 g, 79%), mp 104 °C. Found (calc. for $C_{32}H_{36}N_6S_6Sn_2$): C, 40.8 (41.1); H, 3.9 (3.9); N 9.0 (9.0)%. ^{1}H NMR: δ 8.63 (d, 4H, 2-bipy; ^3J 6.2), 7.69 (d, 4H, 2-Ph; ^3J 8.1), 7.53 (d, 4H, 3-bipy; ^3J 6.2), 7.42 (dd, 4H, 3-Ph; ^3J 7.3/8.1), 7.34 (t, 2H, 4-Ph; ^3J 7.3 Hz), 0.65 (s, 18H, $SnCH_3$), ^2J[^{1}H–^{117,119}Sn] 57.5/59.7 Hz. ^{13}C NMR: δ 186.5 (C–S), 158.6 (C=S), 149.7 (2-bipy), 145.2 (4-bipy), 138.1 (1-Ph), 128.4 (3-Ph), 128.3 (4-Ph), 125.1 (2-Ph), 121.3 (3-bipy), −1.86 ($SnCH_3$), ^1J[^{13}C–^{117,119}Sn] 364.7 Hz (unresolved). ^{119}Sn NMR: δ 77.6. Mössbauer (mm s^{-1}): i.s. 1.34; q.s. 3.15. IR (cm^{-1}): 1595, 1337, 1233, 1071, 1027, 825, 803, 778, 761, 694, 682.

Table 2 Crystal data and structure refinement details for compounds **1**–**3** and **7**–**9**

Compound	**1**	**2**	**3**	**7**	**8**	**9**
Empirical formula	$C_{28}H_{24}N_6S_9Sn$	$C_{28}H_{20}N_4S_6Sn$	$C_{24}H_{28}N_4S_6Sn$	$C_{11}H_{14}N_2S_3Sn$	$C_{16}H_{18}N_3S_3Sn$	$C_{21}H_{26}N_6S_3Sn$
Formula weight	851.76	723.53	683.55	389.11	467.20	577.35
T/K	170(2)	170(2)	170(2)	170(2)	170(2)	170(2)
Crystal system	Monoclinic	Monoclinic	Monoclinic	Triclinic	Triclinic	Monoclinic
Space group	$P2_1/n$	$C2/c$	$P2_1/m$	$P\bar{1}$	$P\bar{1}$	$P2_1/n$
a/Å	15.5450(2)	11.924(1)	7.1380(2)	6.5200(3)	9.5700(3)	14.7340(3)
b/Å	8.61900(10)	21.975(2)	22.9540(6)	7.5280(3)	9.6900(3)	10.6880(2)
c/Å	26.9590(5)	11.255(1)	17.7060(4)	15.3790(5)	12.5000(4)	15.9380(3)
α/°				94.574(3)	105.222(2)	
β/°	104.378(1)	96.340(12)	94.890(1)	95.404(3)	96.477(2)	95.9610(11)
γ/°				94.757(3)	119.362(2)	
U/Å^3	3498.90(9)	2931.1(4)	2891.5(1)	745.97(5)	933.74(5)	2496.30(8)
Z	4	4	4	2	2	4
μ/mm^{-1}	1.298	1.326	1.339	2.113	1.705	1.295
Independent reflections	8001 [R(int) = 0.0602]	2582 [R(int) = 0.0122]	8603 [R(int) = 0.0496]	3393 [R(int) = 0.0418]	4265 [R(int) = 0.0384]	5723 [R(int) = 0.0392]
Goodness-of-fit on F^2	1.042	1.108	0.802	1.028	1.005	0.574
R_1, wR_2 [$I > 2\sigma(I)$]	0.0349, 0.0656	0.0523, 0.1682	0.0404, 0.1188	0.0348, 0.1157	0.0302, 0.0550	0.0241, 0.0679
R_1, wR_2 (all data)	0.0553, 0.0710	0.0533, 0.1687	0.0707, 0.1446	0.0380, 0.1196	0.0407, 0.0589	0.0320, 0.0790

[Di(4-aminopyridine)trimethyltin]$^+$[5-mercapto-3-phenyl-1,3,4-thiadiazoline-2-thionato]$^-$ (9). A large excess of 4-H_2NPy (0.28 g, 3.0 mmol) in diethyl ether (50 ml) was added dropwise to a solution of **7** (0.39 g, 1.0 mmol) in diethyl ether (20 ml). A pale yellow precipitate formed immediately. After stirring for 3 h at room temperature, the solvent was removed and the precipitate was washed with diethyl ether and dried at room temperature, yielding the product as a pale yellow microcrystalline solid (0.51 g, 88%). Alternatively, diethyl ether solutions of the starting materials were allowed to diffuse slowly over 3 days. Slow evaporation of the resultant solution gave the product as a colourless crystalline solid (0.54 g, 93%), mp 136 °C. Found (calc. for $C_{21}H_{26}N_6S_3Sn$): C, 43.8 (43.7); H, 4.6 (4.5); N 14.6 (14.6)%. ^{1}H NMR: δ 7.90 (d, 4H, 2-C_5H_4N; ^3J 5.1), 7.70 (d, 2H, 2-Ph; ^3J 7.3), 7.42 (dd, 2H, 3-Ph; ^3J 7.0/7.7), 7.33 (m, 1H, 4-Ph), 6.75 (s, 4H, NH_2), 6.62 (d, 4H, 3-C_5H_4N; ^3J 5.5 Hz), 0.57 (s, 9H, $SnCH_3$), ^2J[^{1}H–^{117,119}Sn] 66.3 Hz (unresolved). ^{13}C NMR: δ 185.3 (C–S), 172.7 (4-C_5H_4N), 156.5 (C=S), 147.1 (2-C_5H_4N), 139.7 (1-Ph), 128.9 (3-Ph), 128.3 (4-Ph), 126.1 (2-Ph), 109.7 (3-C_5H_4N), 0.00 ($SnCH_3$), ^1J[^{13}C–^{117,119}Sn] 509.0 Hz (unresolved). ^{119}Sn NMR: δ −47.1. Mössbauer (mm s^{-1}): i.s. 1.23; q.s. 3.08. IR (cm^{-1}): 3350, 1635, 1613, 1559, 1518, 1350, 1288, 1234, 1068, 1031, 1007, 837, 829, 772, 760, 697, 664.

Crystallography

Experimental and crystallographic details relating to the structure determination of compounds **1**–**3** and **7**–**9** are given in Table 2. Data for **2** were collected on a CAD4 automatic 4-circle diffractometer, while all the other structures were determined on a Nonius KappaCCD diffractometer.

It became evident in the early stages of refinement of **1** that one of the phenyl rings [C(23)–C(28)] exhibited three-fold positional disorder in the ring plane, which was successfully modelled.

The asymmetric unit in **2** consisted of one half of a molecule, the remaining portion being generated by a 2-fold rotation axis implicit in the space group symmetry. Moreover, in this compound, five of the carbon atoms in one of the phenyl rings [C(9)–C(14)] exhibit disorder in a 1 : 1 ratio with carbons C(902)–C(906) (not shown in Fig. 2). In the final least-squares refinement, restraints were applied to the ADPs of four of these disordered carbons.

In **3**, the asymmetric unit consisted of two independent half-molecules, each seated on a mirror plane. Consequently, two butyl groups on each tin exhibit half site occupancy. In each case, the carbons in one butyl group are seated entirely on the relevant mirror plane, while the additional butyl groups exhibit disorder whereby only the α- and γ-carbons are sited on special positions. The β- and δ-carbons in both cases are disordered in a 1 : 1 ratio on either side of the respective mirror planes straddled by these groups [C(25)–C(28), C(29)–C(32)].

Full matrix anisotropic refinement was implemented in the final least-squares cycles throughout. All data were corrected for Lorentz and polarisation and, with the exception of **3**, for extinction. An absorption correction (multiscan) was applied to data for **1**, **3** **7** and **9**. Hydrogens were included at calculated positions throughout.

CCDC reference numbers 168022–168027.

See http://www.rsc.org/suppdata/dt/b1/b109726a/ for crystallographic data in CIF or other electronic format.

Density functional theory calculations

All calculations were performed using the Gaussian 98 program,[35] employing the B3LYP[36–38] functional in conjunction with the 6-31G* basis set for H, C, N and S,[39] and the SDD energy consistent pseudopotential basis set for Sn.[40] All geometries were fully optimised at the above level using the default optimisation criteria of the program.

Molecular and electronic structure determinations for the systems L^-, LH and $LSnMe_3$ (L = $PhN_2C_2S_3$) were performed under fully relaxed C_1 symmetry. Further calculation of all possible isomers for each system under rigid C_s symmetry revealed the potential energy surfaces to be relatively flat with respect to rotation about the N–C_{ipso} and S–H or S–$SnMe_3$ bonds, but with the C_s solutions being only slightly higher in energy (≤ 11 kJ mol^{-1}) than the optimised C_1 solution in each case. Atomic charges for the C_1 (and C_s) systems were predicted using the natural population analysis (NPA) method implemented within the Gaussian 98 program.[41,42] Atomic charges predicted for the individual C_s isomers were quantitatively very similar to those for the fully relaxed C_1 systems.

Acknowledgements

We thank NATO for support in the form of a travel grant (K. C. M., I. H) and NATO and The Royal Society for a Postdoctoral Fellowship (M. M. V.)

References

1 G. Barone, T. G. Hibbert, M. F. Mahon, K. C. Molloy, L. S. Price, I. P. Parkin, A. M. E. Hardy and M. N. Field, *J. Mater. Chem.*, 2000, **11**, 464.
2 T. G. Hibbert, M. F. Mahon, K. C. Molloy, I. P. Parkin and L. S. Price, *J. Mater. Chem.*, 2001, **11**, 469.
3 I. P. Parkin, L. S. Price, T. G. Hibbert and K. C. Molloy, *J. Mater. Chem.*, 2001, **11**, 1486.

4 S. Bhandari, M. F. Mahon, J. G. McGinley, K. C. Molloy and C. E. Roper, *J. Chem. Soc., Dalton Transactions*, 1998, 3425.
5 I. Haiduc, M. F. Mahon, K. C. Molloy and M. M. Venter, *J. Organomet. Chem.*, 2001, **627**, 6.
6 I. Haiduc and F. T. Edelman, *Supramolecular Organometallic Chemistry*, Wiley-VCH, Weinheim, 1999.
7 R. J. Deeth, K. C. Molloy, M. F. Mahon and S. Whitaker, *J. Organomet. Chem.*, 1992, **430**, 25.
8 J. Bravo, M. B. Cordero, J. S. Casas, A. Sanchez, J. Sordo, E. E. Castellano and J. Zukerman-Schpector, *J. Organomet. Chem.*, 1994, **482**, 147.
9 R. Cea-Olivares, O. Jimenez-Sandoval, G. Espinosa-Perez and C. Silvestru, *J. Organomet. Chem.*, 1994, **484**, 33.
10 R. Cea-Olivares, O. Jiminez-Sandoval, G. Espinosa-Perez and C. Silvestru, *Polyhedron*, 1994, **13**, 2809.
11 M. Barret, S. Bhandari, M. F. Mahon and K. C. Molloy, *J. Organomet. Chem.*, 1999, **587**, 101.
12 A. K. Majunidar and M. M. Chabrabarthy, *Anal. Chim. Acta*, 1958, **19**, 372.
13 A. Kumar, *Z. Anal. Chem.*, 1957, **156**, 265.
14 A. K. Majunidar and M. M. Chabrabarthy, *Z. Anal. Chem.*, 1957, **154**, 262.
15 A. K. Majunidar and M. M. Chabrabarthy, *Z. Anal. Chem.*, 1959, **165**, 100.
16 M. M. Osman, M. A. Makhyoun and A. B. Tadros, *Bull. Soc. Chim. Fr.*, 1980, **11–12**, I.
17 S. A. A. Zaidi and D. K. Varshney, *J. Inorg. Nucl. Chem.*, 1975, **37**, 1804.
18 E. S. Rasper, *Coord. Chem. Rev.*, 1985, **61**, 115.
19 Stauffer Chem., *US Pat.* 3210408, 1965; (*Chem. Abstr.*, 1965, **63**, 13315e).
20 J. M. Williams, J. R. Ferraro, R. J. Thorn, K. D. Carlson, U. Geiser, H. H. Wang, M. Kini and M.-H. Whangbo, *Organic Superconductors (including Fullerenes). Synthesis, Structure, Properties and Theory*, Prentice Hall, Englewood Cliffs, NJ, 1992.
21 M. Hill, M. F. Mahon and K. C. Molloy, *J. Chem. Soc., Dalton Trans.*, 1996, 1857.
22 S. Bhandari, M. F. Mahon and K. C. Molloy, *J. Chem. Soc., Dalton Trans.*, 1999, 1951.
23 K. Yamanari, Y. Kushi, M. Yamamoto, A. Fuyuhiro, S. Kaizaki, T. Kawamoto and Y. Kushi, *J. Chem. Soc., Dalton Trans.*, 1993, 3715.
24 D. K. Srivastava, V. D. Gupta, H. Nöth and W. Rattay, *J. Chem. Soc., Dalton Trans.*, 1988, 1533.
25 I. Lauge, E. Wieland, P. G. Jones and A. Blanchette, *J. Organomet. Chem.*, 1993, **458**, 57.
26 S. S. Batsanov, *J. Mol. Struct.*, 1999, **468**, 151.
27 A. Blaschette, I. Hippel, J. Krahl, E. Wieland, P. G. Jones and A. Siebald, *J. Organomet. Chem.*, 1992, **437**, 279.
28 A. G. Davies, J. P. Goddard, M. B. Hursthouse and N. P. C. Walter, *J. Chem. Soc., Dalton Trans.*, 1986, 1873.
29 W. A. Nuget, R. J. McKinney and R. L. Harlow, *Organometallics*, 1984, **3**, 1315.
30 V. R. Pedireddi, S. Chatterjee, A. Ranganathan and C. N. R. Rao, *J. Am. Chem. Soc.*, 1997, **119**, 10867.
31 A. Ranganathan, V. R. Pedireddi and C. N. R. Rao, *J. Am. Chem. Soc.*, 1999, **121**, 1752.
32 K. C. Molloy, M. F. Mahon, I. Haiduc and C. Silvestru, *Polyhedron*, 1995, **14**, 1169.
33 K. C. Molloy, T. G. Purcell, K. Quill and I. Nowell, *J. Organomet. Chem.*, 1984, **267**, 237.
34 M. Busch, *Chem. Ber.*, 1894, **27**, 2507.
35 M. J. Frisch, G. W. Trucks, H. B. Schlegel, G. E. Scuseria, M. A. Robb, J. R. Cheeseman, V. G. Zakrzewski, J. A. J. Montgomery, R. E. Stratmann, J. C. Burant, S. Dapprich, J. M. Millam, A. D. Daniels, K. N. Kudin, M. C. Strain, O. Farkas, J. Tomasi, V. Barone, M. Cossi, R. Cammi, B. Mennucci, C. Pomelli, C. Adamo, S. Clifford, J. Ochterski, G. A. Petersson, P. Y. Ayala, Q. Cui, K. Morokuma, D. K. Malick, A. D. Rabuck, K. Raghavachari, J. B. Foresman, J. Cioslowski, J. V. Ortiz, A. G. Baboul, B. B. Stefanov, G. Liu, A. Liashenko, P. Piskorz, I. Komaromi, R. J. Gomperts, R. L. Martin, D. J. Fox, T. Keith, M. A. Al-Laham, C. Y. Peng, A. Nanayakkara, M. Challacombe, P. M. W. Gill, B. Johnson, W. Chen, M. W. Wong, J. L. Andres, C. Gonzalez, M. Head-Gordon, E. S. Replogle and J. A. Pople, Gaussian 98, version A9, Gaussian, Inc., Pittsburgh, PA, 1998.
36 A. D. Becke, *Phys. Rev. A: Gen. Phys.*, 1988, **38**, 3098.
37 A. D. Becke, *J. Chem. Phys.*, 1993, **98**, 5648.
38 C. Lee, W. Yang and R. G. Parr, *Phys. Rev. B: Condens. Matter*, 1988, **37**, 785.
39 W. J. Hehre, L. Radom, P. v. R. Schleyer and J. A. Pople, *Ab initio Molecular Orbital Theory*, John Wiley & Sons, Chichester, 1986.
40 A. Bergner, M. Dolg, W. Kuechle, H. Stoll and H. Preuss, *Mol. Phys.*, 1993, **80**, 1431.
41 A. E. Reed, R. B. Weinstock and F. Weinhold, *J. Chem. Phys.*, 1985, **83**, 735.
42 A. E. Reed, L. A. Curtiss and F. Weinhold, *Chem. Rev.*, 1988, **88**, 899.